Analytical, Experimental, and Finite Element Analysis of Buckling and Wrinkling Failure Modes in Carbon/PVC Sandwich Panels

João Alberto Günther Neto, Felipe Ruivo Fuga and Ricardo de Medeiros*

Santa Catarina State University, Centre of Technological Sciences, Department of Mechanical Engineering, Rua Paulo Malschitzki, 200, Joinville, 89219-710, Santa Catarina, Brazil

Abstract: Carbon fibre–reinforced PVC foam sandwich composites are widely used in aeronautical and marine structures due to their high strength-to-weight ratio. However, the stiffness mismatch between face sheets and cores may lead to local buckling modes such as face wrinkling and shear crimping when subjected to compressive loads. Therefore, this study presents a comprehensive investigation on the interaction between global and local buckling modes for sandwich beam structures with lengths varying between 45 and 500 mm subjected to compressive loads, through the comparison of analytical and finite element models using Abaqus® software. Analytical results show a critical force of 3481.1 N and 4017.5N for face sheet wrinkling and shear crimping, respectively. Numerical predictions for both phenomena present a maximum error of approximately 1%, showing that local buckling can be predicted independently of the slenderness ratio of the beam, as suggested by the analytical formulation. However, even for slender beams, the critical buckling load showed a coupling to local behaviour, reducing the corresponding eigenvalue. A maximum deviation of approximately 8% was obtained between analytical and numerical predictions. Finally, an experimental procedure was carried out to observe the associated buckling shapes. As indicated by analytical and numerical predictions, the specimen displayed a local buckling failure mechanism, however, at a much smaller load value related to geometric imperfections and asymmetric boundary conditions. Therefore, the study establishes a validation between analytical and numerical frameworks for predicting local instability failures in CFRP/PVC sandwich structures, providing a tool for engineers to the design of sandwich panels for enhanced structural performance and lightweight and safe components.

Keywords: Composite materials, Buckling, Failure modes, Sandwich structure, Finite element method.

1. INTRODUCTION

Sandwich structures have been widely employed in aerospace, automotive, and marine industries due to their high stiffness-to-weight and strength-to-weight ratios, as well as their excellent energy absorption and thermal insulation capabilities (Allen, 1969; Pokharel and Mahendran, 2024; Zhang *et al.* 2025). These structures typically consist of two stiff face sheets bonded to a lightweight core, which resists transverse shear stresses and prevents local buckling of the faces (Sahu *et al.*, 2022). Through weight reduction combined with high mechanical strength, composite sandwich panels support the design of lightweight yet robust structures (He and Hu, 2008). In aircraft engineering, they are extensively implemented in fuselage coverings, empennage components, and crash-energy absorbers, improving structural longevity, energy efficiency, and safety standards (El-baky *et al.*, 2022; Liang *et al.*, 2023; Sahib and Kovács, 2024). However, under compressive or flexural loading, sandwich structures are susceptible to several failure modes such as face wrinkling, shear crimping, and global buckling, each of which depends on the geometrical configuration, material properties, and boundary conditions (Hoff and Mautner, 1948; Meyer-Piening, 2006; Carlsson and Kardomateas, 2011).

Predicting the onset of failure in sandwich structures has been the focus of analytical, experimental and numerical studies. Analytical approaches, often based on classical beam or plate theories, provide information, however, are limited in capturing the complex interaction between local and global failure mechanisms (Allen, 1969; Hu *et al.*, 2008; Carlsson and Kardomateas, 2011). Consequently, finite element analysis (FEA) has become an alternative for modelling and predicting the mechanical response and failure of composite sandwich structures (Thomsen, 2009; Caliri Jr. *et al.*, 2016). Numerical simulations allow for the inclusion of non-linear effects, material anisotropy, and geometric imperfections, enabling more precise evaluation of structural stability under various loading conditions.

Experimental research has also contributed to understanding the failure mechanisms of sandwich composites. Studies have shown that parameters such as core density, face sheet thickness, and adhesive layer properties strongly affect the compressive and flexural behaviour of the structure (Frostig *et al.*, 1992; Cvitkovich and Jackson, 1999; Daniel and Abot, 2000; Jafarnezhad *et al.*, 2018; Naresh *et al.*, 2023). Experimental campaigns conducted by Allen (1969) and later by Carlsson and Kardomateas (2011) confirmed the presence of distinct buckling modes

*Address correspondence to this author at the Santa Catarina State University, Centre of Technological Sciences, Department of Mechanical Engineering, Rua Paulo Malschitzki, 200, Joinville, 89219-710, Santa Catarina, Brazil; E-mail: ricardo.medeiros@udesc.br

Received on 20-10-2025 Accepted on 17-11-2025 Published on 20-11-2025

E-ISSN: 2311-8717/25

depending on the slenderness ratio and stiffness mismatch between the face sheets and the core. More recent investigations have expanded this analysis, such as, Georges *et al.* (2024) performed analytical and numerical analyses of sandwich panels with lattice cores, identifying distinct local and global buckling behaviours.

Complementary to experimental analysis, computational modelling has focused to capture local and global instability phenomena. Finite element models employing continuum shell and solid elements have been used to predict face wrinkling and core shear failures with high accuracy (Noor *et al.*, 1996; Gdoutos *et al.*, 2003; Hohe and Librescu, 2004). More recent studies have integrated advanced techniques such as numerical homogenization and progressive damage modelling. Likewise, Pozorski *et al.* (2021) reviewed classical and analytical solutions for the instability of sandwich panels, focusing on how displacement assumptions and Poisson's ratio influence wrinkling behaviour. It derives critical stress formulas for orthotropic cores and validates them through numerical analysis. A parametric study highlights how core material properties affect wrinkling stress, emphasizing the combined value of analytical and FE approaches for optimal sandwich design. Kohar *et al.* (2024) modelled two- and multi-phase composites for automotive applications using FEM and the PR375 standard test. Computer simulations in Digimat replaced costly prototyping, enabling rapid optimization of composite components. Results showed that PP/PET/glass fibre composites exhibit significantly higher stiffness than PP/PET/cotton ones, confirming the suitability of glass or carbon fibres for high-strength automotive parts.

Zhang *et al*. (2025) developed a theoretical buckling model for composite laminate sandwich panels by integrating the stress function method with the first-order shear deformation theory (FSDT) to accurately capture the distinct behaviour of laminated composites. The proposed model provides exact closed-form solutions for both global buckling and local wrinkling phenomena. Su and Liu (2025) introduced a structural optimization-based method to address the wrinkling problem in sandwich panels with low computational cost. The wrinkling stress is determined by minimizing the admissible in-plane compressive stress. Validation through finite element simulations and experiments showed good agreement, with discrepancies below 5% and 20%, respectively. Additionally, the method can evaluate wrinkling stress in sandwich panels with functionally graded cores with only a minor increase in computation time.

In this study, the buckling and failure behaviour of carbon fibre reinforced sandwich panels with PVC cores under compression are investigated experimentally and numerically. The results obtained from finite element eigenvalue analyses are compared with analytical predictions and experimental observations, allowing an evaluation of the predominant failure modes and their dependence on specimen geometry. This approach contributes to a better understanding of the mechanical performance of sandwich composites and provides guidance for future structural optimization.

2. MATERIALS AND METHODS

2.1. Specimen Manufacturing

Test specimens were manufactured using VARTM (Vacuum Assisted Resin Transfer Moulding), which consists of layering plies with pre-mixed epoxy resin and hardener over a glass mould and subjecting the assembly to a vacuum under the flexible bag tooling. For the manufacturing of the test specimens the resin and hardener used were, respectively, *E-composites® AR720* and *AH723* with 76% to 24% mass fractions (E-composites®). A sandwich composite structure was manufactured constituted from a single 0.35 mm layer of pre-impregnated carbon fibre, a 10 mm thick expanded PVC core (E-composites® Divinycell H45), followed by another 0.35 mm layer of carbon fibre. A layer of peel ply was placed before the first and after the last layer of carbon fibre to aid the removal of the laminate after curing, and a layer of flow media was placed on the outermost plies to guarantee proper resin flow. A sealing tape was used, along with a plastic bag, to seal the environment over the glass mould. A vacuum pump was attached to the system to keep a pressure of 600 mmHg for 6 hours, and it was then let to cure for 24 hours without external heating. Following this stage, the specimens were cut using a circular saw to a width of 25 mm and two distinct lengths: 50 and 70 mm, and Table **1** presents the final dimensions of the test specimens.

Table 1: Specimens' Final Dimension

Length [mm]	Width [mm]	Thickness [mm]
48.25 ± 0.40	25.73 ± 0.29	10.74 ± 0.05
68.93 ± 0.12		

2.2. Testing Set-Up

Specimens were subjected to compressive mechanical testing following ASTM C364 (ASTM International, 2017), guidelines and the universal testing machine INSTRON EMIC 23-100 with a $100\ kN$ load cell, shown in Figure **1**.

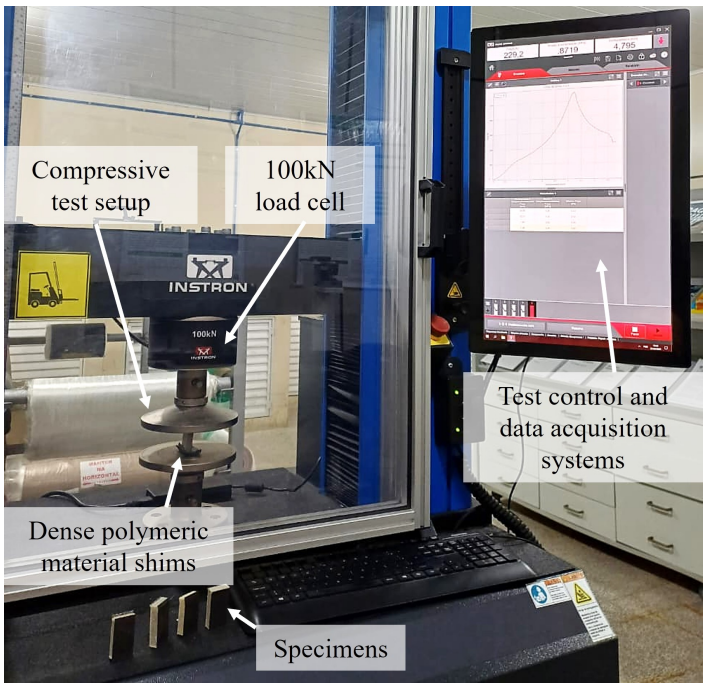

Figure 1: Universal testing machine used for the experiments.

To mitigate manufacturing inconsistencies in specimen's length limiting the parallelism between faces at the end of the composites, a dense polymer material was used between the specimens and the compressive plates, in an attempt to redistribute the compressive loads, as displayed in Figure **1**. As the assembly consists of elastic bodies and shims in a series configuration, the apparent stiffness is affected by the polymeric material elastic properties. However, for the maximum load analysis, the additional material does not contribute, as it is related to the sandwich component behaviour. The crosshead displacement rate was 2 mm/min, and the outputs acquired from testing were the load (N) and displacement (mm) signals throughout time.

2.3. Finite Element Model

A numeric model of the compression test was developed using the Abaqus® Finite Element (FE) software with the objective of capturing the loads corresponding to the start of the instability phase of multiple specimens, as a function of the length. Therefore, a linear buckling analysis was implemented so that the different buckling shapes could be evaluated for each specimen configuration, varying from local instabilities such as shear crimping and face sheet wrinkling to global buckling modes. FE model boundary conditions are shown in Figure **2**, where fixed surfaces were prescribed at the end of the beam's

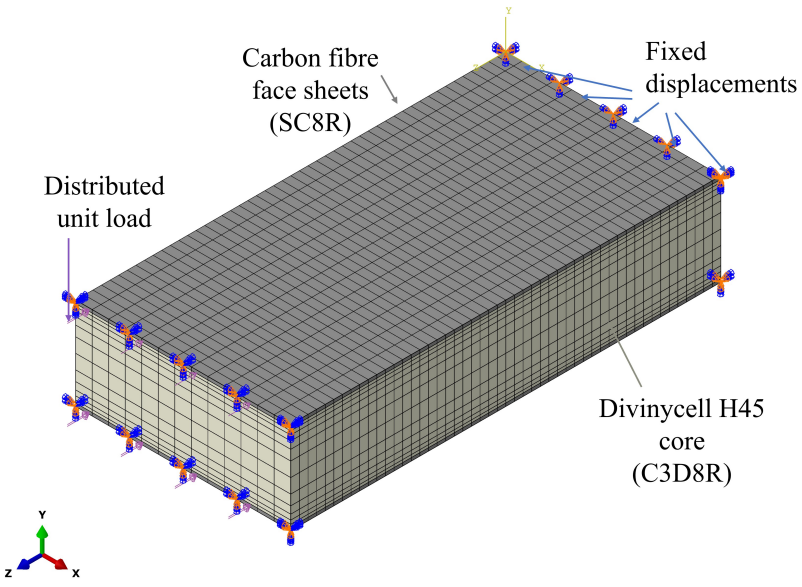

Figure 2: Boundary conditions used in the simulations.

longitudinal direction. Specimen dimensions were taken from the average experimental values.

As the composite material consists of carbon fibre face sheets coupled to a soft core, different element types were used to represent each section. The core was modelled with hexahedral three-dimensional elements (C3D8R) with eight nodes and reduced integration due to the necessity to capture the through-the-thickness deformations in the core. However, due to the small thickness associated with the carbon fibre face sheets, three-dimensional continuum shell elements (SC8R) with eight nodes and reduced integration were used. For this element formulation kinematic restrictions related to the Reissner-Mindlin plate model are applied to solid elements, thus resulting in a continuum hexahedral element without changes in the through-the-thickness dimension. A unit load of 1N was applied as a distributed pressure over the face sheets as displayed in Figure **2**.

The properties used in the model are displayed in Table **2** and were taken from Günther Neto *et al* (2025) for the carbon fibre, where a complete characterisation of the effective sandwich structure properties was conducted for specimens under bending.

Table 2: Material Properties - Günther Neto *et al.* (2025)

	CFRP	Core Divinycell H45
$\mathbf{E}_{xx} = E_{zz}$ [MPa]	13000.00	50.00
G_{xz} [MPa]	4000.00	16.70
ν_{xz}	0.06	0.49

For the analysis, the first 50 eigenvalues and mode shapes obtained through using the Lanczos eigenvalue solution algorithm. The lowest energy eigenmodes related to each distinct failure modes were recorded and compared.

A mesh independence study was carried out to ensure that the results are not depended on mesh size. For this, four different mesh sizes ranging from 1.00 to 0.25 mm were analysed and the eigenvalues corresponding to each failure mode being studied were extracted, being: global buckling (P_{cr}), face sheet wrinkling (P_{wr}) and shear crimping (P_{crimp}). As presented in Table **3**, the greatest relative difference (e) between each mesh size's is less than 0.50%. Therefore, the decision was made to carry out all simulations with a mesh size of 0.25 mm.

2.4. Analytical Model

The analytical investigation of local instability in sandwich panels is based on classical buckling theory and on established formulations developed to predict both global and local modes of instability. In particular, three main failure modes are considered: global buckling (Euler type), local face sheet wrinkling, and shear crimping. Each mode can be expressed through closed-form equations derived from elasticity theory and stability analysis.

The global buckling mode of a sandwich beam or panel can be approximated by the classical Euler equation,

$$P_{buck} = \frac{\pi^2 (EI)_{eq}}{(kL)^2} = \frac{\pi^2 b D_{11}}{(kL)^2} \quad (1)$$

considering the effective bending stiffness $(EI)_{eq}$, the length L, and the boundary condition factor k. For sandwich panels the bending stiffness can be expressed in terms of section bending stiffness matrix $\boldsymbol{D}$ component evaluated along the beam's length direction and the width b. In fact, this equation defines the upper limit of the critical load for global instability and is valid when the structural slenderness is sufficiently high, so that flexural deformation dominates the response.

For local instabilities, where deformations occur within the faces over a length scale comparable to the core thickness, face sheet wrinkling becomes the dominant mode. According to the model proposed by Hoff and Mautner (1945) and later consolidated in the NASA report by Ley *et al.* (1999), the critical wrinkling load depends on the elastic properties of the faces and the core, and can be expressed as

$$P_{wr} = 0.91 t b \left(E_f E_c G_c\right)^{1/3} \quad (2)$$

where *t* is the total thickness of face sheet layers, *b* the panel width, E_f the Young's modulus of the face sheet, E_c the through-thickness Young's modulus of the core,

Table 3: Mesh Independence study – Load Values in [N]

Mesh size [mm]	P_{cr}	|e| [%]	P_{wr}	|e| [%]	P_{crimp}	|e| [%]
1.00	4171.9	-	3506.9	-	4087.2	-
0.75	4166.8	0.12	3490.6	0.47	4081.9	0.13
0.50	4172.3	0.13	3479.7	0.31	4090.3	0.21
0.25	4171.0	0.03	3473.5	0.18	4089.0	0.03

and G_c the core shear modulus. This relation is derived from an analogy between the compressed face sheet and a thin plate resting on an elastic foundation representing the core. The coefficient 0.91 was obtained from the analytical solution of the symmetric wrinkling mode proposed by Hoff and Mautner (1945), which was later confirmed experimentally for thick solid cores.

However, when the core exhibits significant shear flexibility, global buckling instability may occur coupled to shear crimping, characterised by relative shear deformation between the upper and lower faces. In this case, the crimping critical load can be estimated as

$$P_{crimp} = G_c h_c b. \quad (3)$$

Equation (3) represents the lower limit of the critical load and is associated with short-wavelength antisymmetric deformation modes, where localized shear distortion in the core dominates the failure mechanism. As discussed by Ley *et al.* (1999), the shear crimping mode can be interpreted as a special case of short-wavelength wrinkling. Finally, the effective critical load computed as a function of the global buckling and crimping instabilities as

$$\frac{1}{P_{cr}} = \frac{1}{P_{buck}} + \frac{1}{P_{crimp}}. \quad (4)$$

Comparing these three formulations, it was possible to conclude that the overall stability behaviour of sandwich panels arises from the interaction between the elastic properties of the faces and the core. While the term E governs the global buckling response, the combined parameter $\left(E_f E_c G_c\right)^{1/3}$ and the shear modulus G_c control local instability phenomena such as wrinkling and shear crimping. This analytical framework thus provides practical information for predicting the critical failure mode and corresponding load, as well as for validating and calibrating numerical and experimental results.

3. RESULTS AND DISCUSSIONS

3.1. Finite Element Result

The eigenvectors corresponding to the different failure modes are illustrated in Figures **3** and **4**, while the respective eigenvalues are presented in Figure **5**. Mode shapes are displayed for two distinct sandwich panel lengths corresponding to 50 and 120 mm. In the image, the distinction between global and local buckling loads can be made, where the wrinkling instability is characterized by a symmetric face sheet dominated behaviour, while the crimping displays a core dominated buckling shape, with a sharp transverse displacement value.

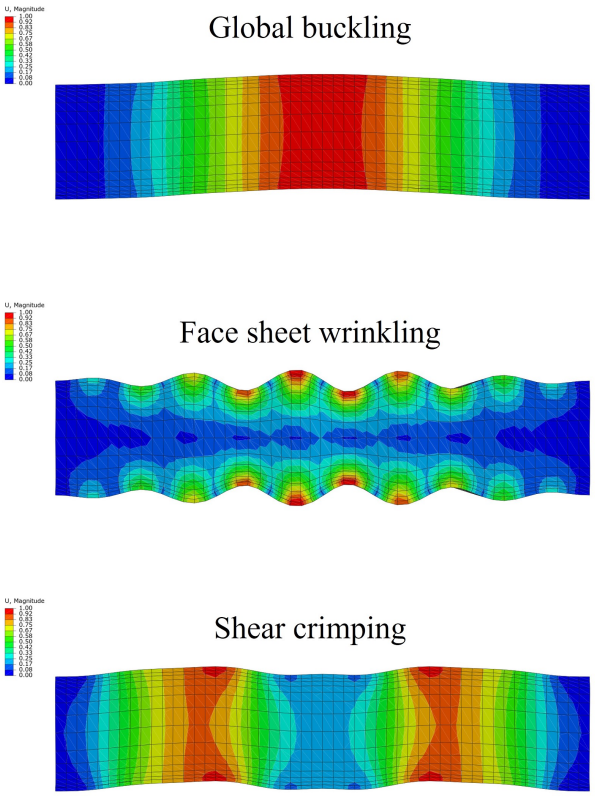

Figure 3: Mode shapes for $L = 50mm$

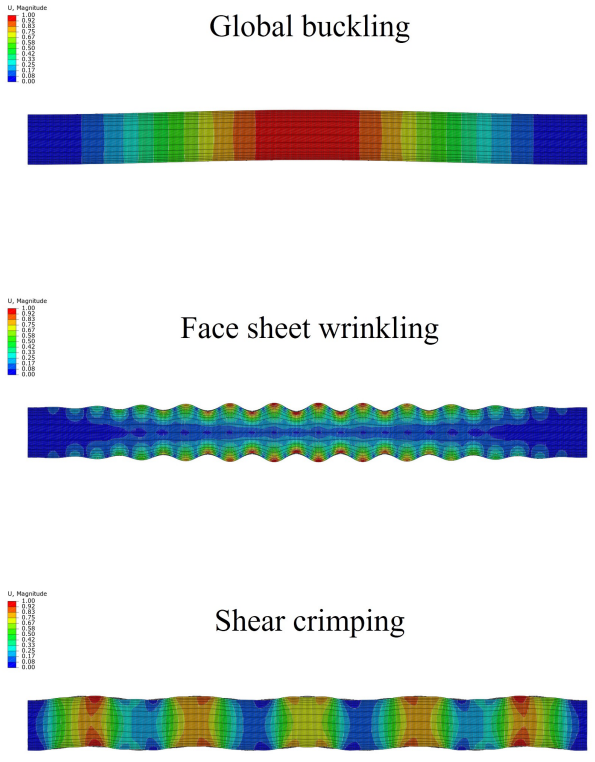

Figure 4: Mode shapes for $L = 120mm$

Buckling loads associated with each failure mode characteristics are displayed in Figure **5** for models with different slenderness ratio. In addition, analytical solutions are overlayed on the numerical results,

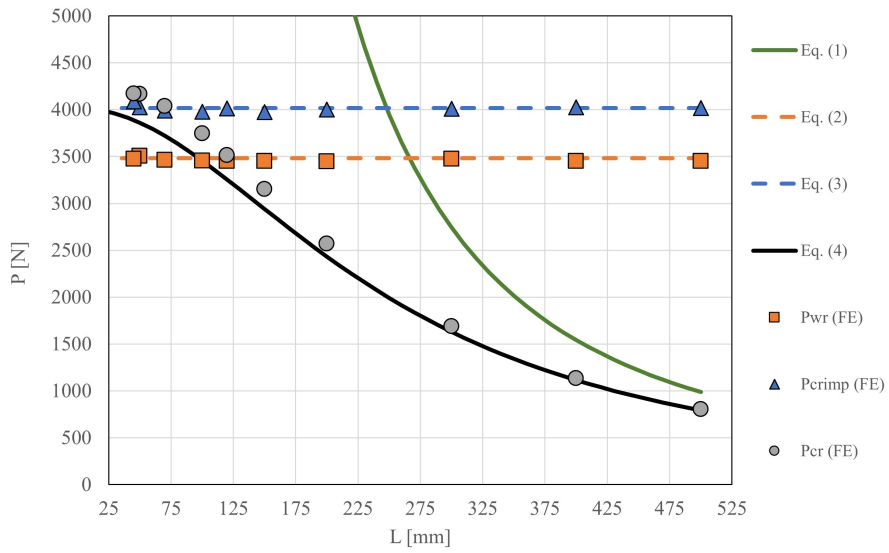

Figure 5: Eigenvalues as a function of length.

represented by dashed and continuous lines in the image. For slender beams ($L \to \infty$) the global buckling load approaches Euler's predictions from Eq. (1). In contrast, for all specimen lengths the eigenvalue associated with both wrinkling and crimping modes displayed an approximately constant value, indicating that the mode is indeed independent of the slenderness ratio. Furthermore, compared to numerical predictions, the values obtained from Eqs. (2) and (3) provided accurate results, with a maximum deviation of 1.7% for the crimping mode at $L = 45mm$.

Despite the validity of Euler's solution as the slenderness ratio increases, Figure **5** shows that the global buckling load value is significantly lower than predictions using Eq. (1) for intermediate length values. Therefore, numerical results suggest an interaction between global and local buckling modes. Interestingly, Eq. (4) provided accurate predictions for the coupled instability of global and crimping buckling modes, with a maximum deviation of 8% for the length of 70 mm.

Table **4** displays a comparison between analytical and FE results for different length values and the corresponding deviations. For the computation of analytical predictions the values displayed in Table **2** were used, with $b = 25\ mm, t = 0.35\ mm$ and $h_c = 10\ mm$, resulting in a bending stiffness $D_{11} = 2.50(10^5)\ N \cdot mm$. Furthermore, boundary conditions were assumed as clamped ends with $k = 0.5$. Results show that crimping eigenvalue solutions displayed the greatest deviation values with relative differences under 8%.

3.2. Experimental Results

The experimental load-displacement curves are shown in Figure **6** for specimens with $L = 50mm$ and $L = 70mm$. The critical load is taken as the maximum value, with the average values shown in Table **5**.

Table 4: Relative Difference between Analytical and FEM Results – Load Values in [N]

L [mm]	Eq. (1)	P_{wr}	Eq. (2)	e [%]	P_{crimp}	Eq. (3)	e [%]	P_{cr} (FE)	Eq. (4)	e [%]
500	987.8	3451.5	3481.1	-0.9%	4015.4	4017.5	-0.1%	803.7	792.9	1.3%
400	1543.4	3451.7	3481.1	-0.9%	4025.5	4017.5	0.2%	1133.4	1115.1	1.6%
300	2743.9	3473.8	3481.1	-0.2%	4009.8	4017.5	-0.2%	1688.8	1630.4	3.5%
200	6173.7	3448.7	3481.1	-0.9%	4001.9	4017.5	-0.4%	2568.3	2433.8	5.2%
150	10975.5	3450.2	3481.1	-0.9%	3975.7	4017.5	-1.1%	3150.5	2941.0	6.7%
120	17149.2	3452.2	3481.1	-0.8%	4012.7	4017.5	-0.1%	3514.0	3255.0	7.4%
100	24694.8	3454.8	3481.1	-0.8%	3979.4	4017.5	-1.0%	3744.4	3455.4	7.7%
70	50397.6	3462.5	3481.1	-0.5%	3988.0	4017.5	-0.7%	4038.7	3720.9	7.9%
50	98779.3	3505.7	3481.1	0.7%	4025.2	4017.5	0.2%	4165.5	3860.5	7.3%
45	121949.8	3473.5	3481.1	-0.2%	4089.0	4017.5	1.7%	4171.0	3889.4	6.8%

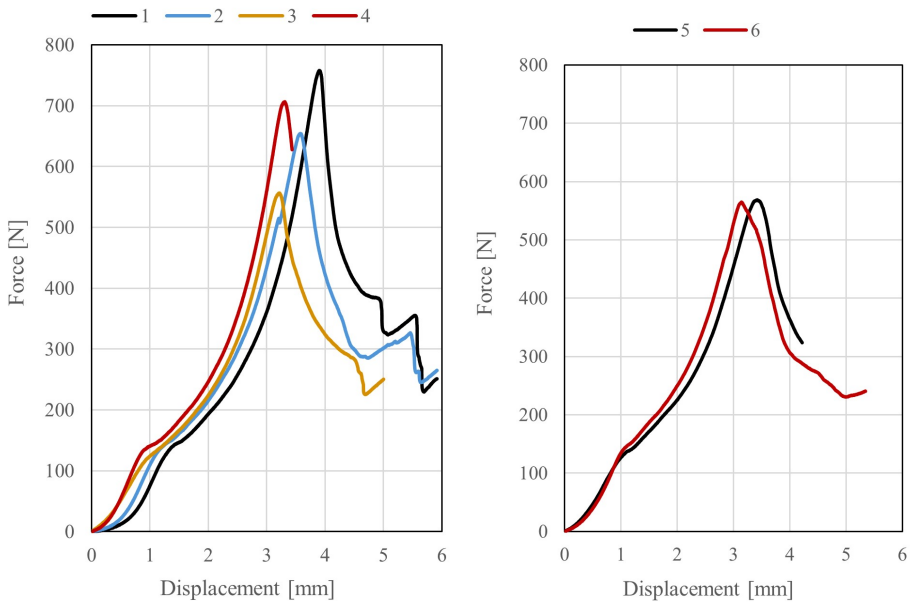

(**a**) 50 mm specimens (**b**) 70 mm specimens

Figure 6: Experimental load-displacement curves.

Table 5: Experimental Average Maximum Compressive Load

Length [mm]	Maximum Load [N]
50	668.88
70	566.85

For all specimens, the observed failure mode resembles the shear crimping shape, assuming that failure occurs at a single cross-sectional position. Failure characteristics of a representative specimen are displayed in Figure **7**.

However, the observed failure mode can also be related to the boundary conditions imposed on the experimental testing procedure, that might not capture the theoretical clamped constraint. FE predictions for different boundary conditions, such as clamped-simply supported beams, lead to different lower energy local buckling shapes such as the solution displayed in Figure **8**. Despite the mode shape correlation, the associated critical load value of 2023.9 N predicted by the numerical model is still much greater than the experimentally observed maximum load value.

As mentioned by Ley *et al.* (1999), crimping related failure in sandwich composites under compressive loads can occur at load values much smaller than the analytical and numerical predictions, mainly due to imperfection on the geometry leading to waviness in the face sheets. Moreover, to ensure proper boundary conditions, the end of the test specimens must be cut to parallel flat planes that is often unobtainable. Therefore, for further understanding of local and global buckling instabilities on sandwich composite structures the introduction of imperfect geometry and asymmetric boundary conditions is required.

3.3. Discussion

The agreement between FE predictions and analytical models for the critical load validate the theoretical framework relating to three different

Figure 7: Experimental failure mode.

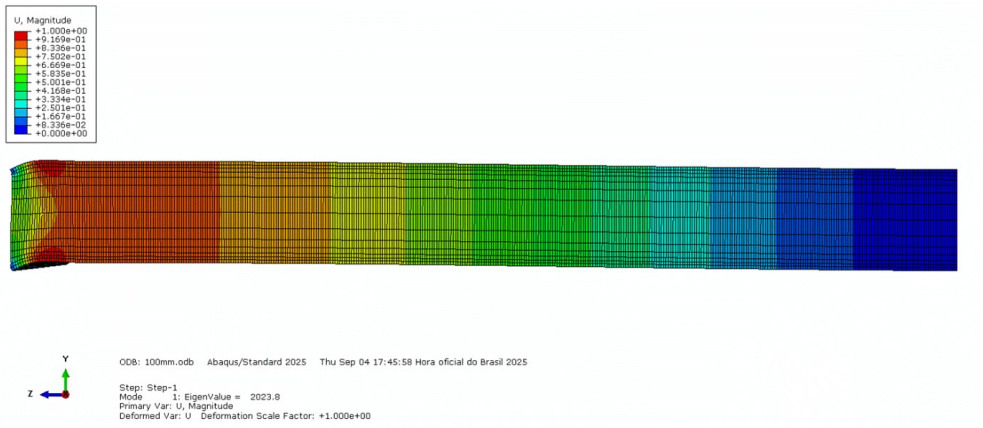

Figure 8: Lower energy eigenshape for clamped-simple support boundary conditions.

instability modes. While the models indicate that the shear crimping occurs at a higher load compared to the global buckling and face sheet wrinkling, the global buckling modes displayed an interaction with crimping failure, differing substantially from Euler's column buckling formulation. Therefore, for short beams, a combination of global buckling and shear crimping failure modes were expected and observed on the experimental testing campaign. Moreover, the models confirm that local instabilities are related to the mismatch in material properties between face sheet and core constituents and influence global instability threshold values.

The difference between experimental maximum load and analytical/numerical predictions indicates that the representation of the actual testing conditions is not properly described by the model assumptions. As shown in Figure **8**, the alleviation of the rotational constraint for one edge in the numerical model predicts a crimping load of 2023 [N] for a 100 mm beam, while the clamped condition yields 3454 [N], representing a 41.4% reduction in the critical load value. Moreover, geometrical imperfection was not accounted for in both analytical and FE formulations, which is impractical for experimental applications. As discussed in Section 3.1, local instabilities are not related to boundary conditions and are dependent on the mismatch between material properties on the sandwich structure. However, the global buckling shape showed a strong dependency on both Euler's column buckling and shear crimping predictions. Therefore, as the increase in imperfection lowers the global buckling load, a reduction in the coupled P_{cr} value is expected.

Finally, while the current work involves non-biodegradable Carbon/PVC sandwich panels for high-performance applications, the validated analytical and numerical methodology is applicable to the design of sustainable composite structures. This study complements the performance comparison between synthetic and natural fibres in sandwich structures under bending presented in Günther Neto *et al* (2025), where wrinkling instabilities were observed for the synthetic fibres only, as the mismatch between core and face sheet properties are significant. Therefore, the methodology showed in this study indicates can be transferred to natural fibres, where the effects of local instabilities might not be as relevant as synthetic fibres. Moreover, the results and methodology presented in this study are consistent with recent guidelines for the development of sustainable epoxy composites containing dynamic bonds, as discussed by Wang *et al*. (2025), reinforcing the potential integration between traditional instability analyses and advances in recyclable, bio-based epoxy matrices.

4. CONCLUSION

Through analytical, experimental and numerical methods, this work evaluated the effect of instabilities induced compressive loads on composite sandwich beams. In essence, the following conclusions were observed:

- Coupling of global buckling and shear crimping can be accurately predicted by the analytical formulation.
- FE models indicated that wrinkling and shear crimping are indeed independent of the sandwich beam length.
- Shear dominated core failure modes were observed on the experiments conducted.
- Critical loads obtained experimentally are significantly lower than the numerical and analytical instability load predictions.
- The alleviation of constraints in the numerical model resulted in buckling shapes related to the experimental failure mode.

Therefore, this study contributes with an in-depth description of the associated local buckling prediction analytical and numerical tools with practical use on the design of compressive loaded composite structures for the naval and aviation industries. The authors recommend further development on the characterisation of the effect of different boundary conditions through experimental testing and numerical modelling of the impact of imperfect geometry under compressive loads.

ACKNOWLEDGEMENT

The authors gratefully acknowledge the financial support of the Santa Catarina State Research and Innovation Foundation (FAPESC numbers: 2017TR1747, 2021TR843, 2023TR563, and 2024TR2327). As well as from the Coordination for the Improvement of Higher Education Personnel (CAPES Funding Code 001). Ricardo De Medeiros acknowledges the financial support of the National Council for Scientific and Technological Development (CNPq grant number: 304795/2022-4). Felipe Ruivo Fuga acknowledges the financial support of the National Council for Scientific and Technological Development (CNPq grant number: 385856/2024-5).

CONFLICTS OF INTEREST

The authors declare that they have no known competing financial interests or personal relationships that could have appeared to influence the work reported in this paper.

REFERENCES

[1] ASTM International (2017). C364-99, Standard Test Method for Edgewise Compressive Strength of Sandwich Constructions. American Society for Testing Materials International. West Conshohocken, PA.

[2] Allen, H. G. (1969). Analysis and design of structural sandwich panels. Pergamon Press, Oxford, UK. https://doi.org/10.1016/B978-0-08-012870-2.50006-7

[3] Caliri Jr., M.F., Ferreira, A.J. & Tita, V. (2016). A review on plate and shell theories for laminated and sandwich structures highlighting the Finite Element Method. Composite Structures, 156, 63-77. https://doi.org/10.1016/j.compstruct.2016.02.036

[4] Carlsson, L.A. & Kardomateas, G.A. (2011). Structural and failure mechanics of sandwich composites, Vol. 121. Springer Science & Business Media: Dordrecht. https://doi.org/10.1007/978-1-4020-3225-7

[5] Cvitkovich, M.K. & Jackson, W.C. (1999). Compressive failure mechanisms in composite sandwich structures. Journal of the American Helicopter Society, 44(4), 260-268. https://doi.org/10.4050/JAHS.44.260

[6] Daniel, I.M. & Abot, J.L. (2000). Fabrication, testing and analysis of composite sandwich beams. Composites Science and Technology, 60(12-13), 2455-2463. https://doi.org/10.1016/S0266-3538(00)00039-7

[7] El-baky, M.A.A., Allah, M.M.A., Kamel, M. & Abd-Elaziem, W. (2022). Lightweight cost-effective hybrid materials for energy absorption applications. Scientific Reports, 12(1): 21101. https://doi.org/10.1038/s41598-022-25533-3

[8] Frostig, Y., Baruch, M., Vilnay, O. & Sheinman, I. (1992). High-order theory for sandwich-beam behavior with transversely flexible core. Journal of Engineering Mechanics, 118(5), 1026-1043. https://doi.org/10.1061/(ASCE)0733-9399(1992)118:5(1026)

[9] Gdoutos, E.E., Daniel, I.M. & Wang, K.A. (2003). Compression facing wrinkling of composite sandwich structures. Mechanics of materials, 35(3-6), 511-522. https://doi.org/10.1016/S0167-6636(02)00267-3

[10] Georges, H., Becker, W. & Mittelstedt, C. (2024). Analytical and numerical analysis on local and global buckling of sandwich panels with strut-based lattice cores. Archive of Applied Mechanics, 94(8), 2269-2283. https://doi.org/10.1007/s00419-024-02636-z

[11] Günther Neto, J.A., Scheffer, W.C., Fuga, F.R. & De Medeiros, R. (2025). Mechanical Characterization of Natural and Synthetic Fibres using Sandwich Structures Under Bending. Journal of Modern Mechanical Engineering and Technology, 12, 34-44. https://doi.org/10.31875/2409-9848.2025.12.05

[12] He, M. & Hu, M. (2008). A study on composite honeycomb sandwich panel structure. Materials & Design, 29(3), 709-713. https://doi.org/10.1016/j.matdes.2007.03.003

[13] Hoff, N.J. & Mautner, S.E. (1948). Bending and Buckling of Sandwich Beams. Journal of the Aeronautical Sciences, 15(12), 707-720. https://doi.org/10.2514/8.11699

[14] Hohe, J. & Librescu, L. (2004). Advances in the structural modeling of elastic sandwich panels. Mechanics of Advanced Materials and Structures, 11(4-5), 395-424. https://doi.org/10.1080/15376490490451561

[15] Hu, H., Belouettar, S., Potier-Ferry, M. & Daya, E.M. (2008). Review and assessment of various theories for modeling sandwich composites. Composite Structures, 84(3), 282-292. https://doi.org/10.1016/j.compstruct.2007.08.007

[16] Jafarnezhad, S., Shalbafan, A. & Luedtke, J. (2018). Effect of surface layers compressibility and face-to-core-layer ratio on the properties of lightweight hybrid panels. International Wood Products Journal, 9(4), 164-170. https://doi.org/10.1080/20426445.2018.1546979

[17] Kohar, R., Miskolci, J., Pompas, L., Kucera, L., Stevko, P., Petru, M. & Mishra, R.K. (2024). Computational Analysis of Mechanical Properties in Polymeric Sandwich Composite Materials. Polymers, 16(5), 673. https://doi.org/10.3390/polym16050673

[18] Ley, R.P., Lin, W. & Mbanefo, U. (1999). Facesheet wrinkling in sandwich structures. Technical Report, CR-1999-208994, NASA Center for AeroSpace Information. Northrop Grumman Corporation, El Segundo, California, USA.

[19] Liang, K., Li, Z., Wang, Z. & Zhang, Y. (2023). The thermal-mechanical buckling and postbuckling design of composite laminated plate using a ROM-driven optimization method. Mechanics of Advanced Materials and Structures, 30(19), 3847-3861. https://doi.org/10.1080/15376494.2022.2084578

[20] Meyer-Piening, H.-R. (2006). Sandwich Plates: Stresses, Deflection, Buckling and Wrinkling Loads - A Case Study. Journal of Sandwich Structures & Materials, 8(5), 381-394. https://doi.org/10.1177/1099636206064825

[21] Naresh, K., Alia, R.A., Cantwell, W.J., Umer, R. & Khan, K.A. (2023). Influence of face sheet thickness on flexural strength characteristics of carbon/epoxy/Nomex honeycomb sandwich panels. Journal of Sandwich Structures & Materials, 25(5), 537-554. https://doi.org/10.1177/10996362231159925

[22] Noor, A.K., Burton, W.S. & Bert, C.W. (1996). Computational models for sandwich panels and shells. Applied Mechanics Reviews, 49(3): 155-199. https://doi.org/10.1115/1.3101923

[23] Pokharel, N. & Mahendran, M. (2024). Finite element analysis and design of sandwich panels subject to local buckling effects. Thin-Walled Structures, 42(4), 589-611. https://doi.org/10.1016/j.tws.2003.08.002

[24] Pozorski, Z., Pozorska, J., Kreja, I. & Smakosz, Ł. (2021). On wrinkling in sandwich panels with an orthotropic core. Materials, 14(17), 5043. https://doi.org/10.3390/ma14175043

[25] Sahib M.M. & Kovács G. (2024). Multi-objective optimization of composite sandwich structures using artificial neural networks and genetic algorithm. Results in Engineering, 21, 101937. https://doi.org/10.1016/j.rineng.2024.101937

[26] Sahu, S.K., Sreekanth, P.S.R. & Reddy, S.V.K. (2022). A Brief Review on Advanced Sandwich Structures with Customized Design Core and Composite Face Sheet. Polymers, 14(20), 4267. https://doi.org/10.3390/polym14204267

[27] Su, W. & Liu, S. (2025). New method for predicting the wrinkling stress in sandwich panels. Archive of Applied Mechanics, 95(1), 4. https://doi.org/10.1007/s00419-024-02718-y

[28] Thomsen, O.T. (2009). Sandwich materials for wind turbine blades—present and future. Journal of Sandwich Structures & Materials, 11(1), 7-26. https://doi.org/10.1177/1099636208099710

[29] Wang, Y., Jian, X. & Weng Z. (2025). Progress in structural design and multifunction of bio-based epoxy resin composites containing dynamic bonds. Journal of Composites and Biodegradable Polymers, 13, 90-108. https://doi.org/10.12974/2311-8717.2025.13.07

[30] Zhang, Y., Liu, Q. & Chen, L. (2025). Buckling modeling and numerical validation of composite panels for sandwich structures. Journal of Sandwich Structures & Materials, 27(6), 10996362251334038. https://doi.org/10.1177/10996362251334038

https://doi.org/10.12974/2311-8717.2025.13.08